

## Pseudogap and Spin Fluctuations in the Normal State of the Electron-Doped Cuprates

B. Kyung,<sup>1</sup> V. Hankevych,<sup>1,2</sup> A.-M. Daré,<sup>3</sup> and A.-M. S. Tremblay<sup>1</sup>

<sup>1</sup>*Département de Physique and RQMP, Université de Sherbrooke,  
Sherbrooke, Québec, Canada J1K 2R1*

<sup>2</sup>*Department of Physics, Ternopil State Technical University, 56 Rus'ka Street, UA-46001 Ternopil, Ukraine*

<sup>3</sup>*L2MP, CNRS, Université de Provence, 49 rue Joliot Curie, BP 146, 13384 Marseille, Cedex 13, France*

(Received 22 December 2003; published 29 September 2004)

We present reliable many-body calculations for the  $t$ - $t'$ - $t''$ - $U$  Hubbard model that explain in detail the results of recent angle-resolved photoemission experiments on electron-doped high-temperature superconductors. The origin of the pseudogap is traced to two-dimensional antiferromagnetic spin fluctuations whose calculated temperature-dependent correlation length also agrees with recent neutron scattering measurements. We make specific predictions for photoemission, for neutron scattering, and for the phase diagram.

DOI: 10.1103/PhysRevLett.93.147004

PACS numbers: 74.72.-h, 71.10.Fd, 71.27.+a, 79.60.-i

High-temperature superconductors (HTSC) still present one of the main contemporary challenges to condensed matter physics. While single-particle excitations, in the standard theory, are described by the quasiparticle (Fermi liquid) concept, that approach fails in HTSC. Quasiparticles can disappear altogether on certain segments of the would-be Fermi surface [1]. This in turn leads to anomalous properties in transport and in thermodynamic data that are collectively referred to as pseudogap phenomena. Pseudogap phenomena occur both in hole-doped ( $h$ -doped) cuprates and in the electron-doped ( $e$ -doped) ones. Although the majority of research has focused on  $h$ -doped materials, experimental activity on  $e$ -doped cuprates has been steadily increasing in the last few years, as the community realizes the importance of looking at the big picture for HTSC. Strong electron-electron interactions and low dimensionality are the main stumbling blocks for theories of HTSC. In this context, one can argue that it is the lack of controlled theoretical approximations and consequent lack of quantitative predictions and detailed agreement with experiment that are the main reasons why there is no consensus on the correct theory in this field. We show in this Letter that the somewhat weaker coupling in  $e$ -doped HTSC leads to an unprecedented opportunity to obtain a detailed agreement between theory and experiment.

We use the single-band Hubbard model on a square lattice, which contains a repulsive local interaction  $U$  and a kinetic contribution of bandwidth  $W$  that is fitted to band structure using nearest  $t$ , second-nearest  $t'$ , and third-nearest  $t''$  neighbor hoppings. Reliable calculations for the Hubbard model can be done when the expansion parameter  $U/W$  becomes less than unity. As was pointed out by several groups [2–5], this is precisely the situation that occurs in  $e$ -doped HTSC as doping is increased towards optimal doping. Smaller values of  $U/W$  physically come from better screening in  $e$ -doped systems [5]. Note that the pseudogap mechanism discussed here can be different from that occurring at strong coupling [5].

We calculate the momentum  $\vec{k}$  and energy  $\omega$  dependent single-particle spectral weight  $A(\vec{k}, \omega)$  and find that it is in detailed agreement with angle-resolved photoemission spectroscopy (ARPES) on  $\text{Nd}_{2-x}\text{Ce}_x\text{CuO}_4$  [1,6,7]. In particular, we explain the pseudogap observed in  $e$ -doped cuprates at binding energies of the order of a few hundred meV. To show that we correctly handle the physics of antiferromagnetic (AFM) fluctuations that is behind that pseudogap, we successfully compare our temperature-dependent correlation length to that measured by neutron scattering on  $\text{Nd}_{2-x}\text{Ce}_x\text{CuO}_4$  [8,9]. None of the recent theoretical works on  $e$ -doped cuprates [2–5,10,11] have obtained momentum, frequency, as well as temperature dependent properties that are in detailed agreement with both ARPES and neutron data. We also find good estimates for the Néel temperature [8] and for the  $d$ -wave superconducting transition temperature [12]. A few of our predictions follow: (i) The ARPES pseudogap disappears with increasing temperature when the AFM correlation length  $\xi$  becomes smaller than the single-particle thermal de Broglie wavelength  $\xi_{\text{th}}$ . The corresponding pseudogap temperature  $T^*$  is close to that found in optical experiments [13]. (ii) In the pseudogap regime, the characteristic spin fluctuation energy in neutron scattering experiments is smaller than the thermal energy (renormalized classical regime) and the spin fluctuations are overdamped near the pseudogap temperature. (iii) There is no large energy ( $\geq 100$  meV) pseudogap at dopings larger than that of the quantum critical point (QCP), whose location we also calculate and which coincides with that observed experimentally for the antiferromagnetic to paramagnetic QCP [8,14].

Since we are in a nonperturbative regime, even with  $U/W \lesssim 1$ , calculations are still a challenge. We use the nonperturbative two-particle self-consistent (TPSC) approach valid in that regime. The reasons are as follows: TPSC satisfies at the same time the Pauli principle, the Mermin-Wagner theorem, and has a self-energy that is

consistent with the sum-rule relating potential energy to single-particle properties [15–18]. By contrast with other approaches [4], TPSC also automatically takes into account quantum fluctuations that renormalize  $U$  (Kanamori screening). Results for the charge and spin structure factors, spin susceptibility, and double occupancy obtained with the TPSC scheme satisfy conservation laws. As a theory then, TPSC fulfills crucial physical constraints. In addition, the above quantities have been found to be in quantitative agreement with quantum Monte Carlo (QMC) calculations and other numerical methods [15–20] for both the nearest-neighbor [15,16] and next-nearest-neighbor [19] Hubbard models in two dimensions. In particular, the agreement with QMC calculations for single-particle properties has been verified [16,17,20] even as we enter the pseudogap regime at low enough temperature. An internal accuracy check [16] allows one to decide on the validity of the results in cases where QMC or other exact results are not available as references. We do not consider the case of very large correlation length, where the quantitative details of TPSC become less accurate. Therefore, we are always within the domain where the approach is reliable.

*Energy dispersion curves.*—One of the most striking features of ARPES results in optimally  $e$ -doped cuprates is the disappearance of  $\omega = 0$  excitations near the intersection of the noninteracting Fermi surface with the AFM zone boundary. These pseudogapped points in the Brillouin zone are called hot spots. Band structure parameters that are input in the calculation have to lead to

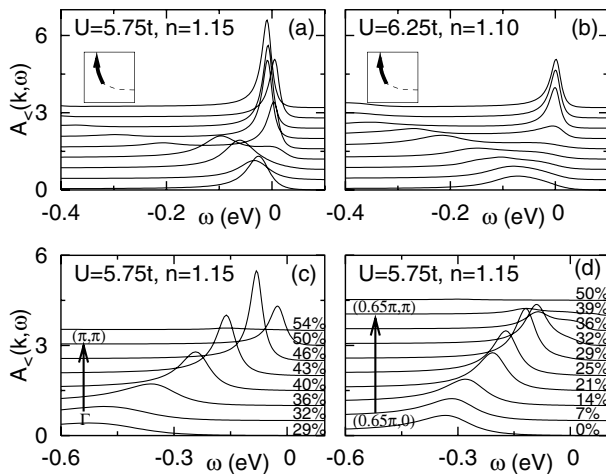


FIG. 1. Energy distribution curves  $A_<(\vec{k}, \omega) \equiv A(\vec{k}, \omega)f(\omega)$  along the Fermi surface shown in the insets for (a)  $n = 1.15$ ,  $U = 5.75t$  and (b)  $n = 1.10$ ,  $U = 6.25t$ . Lines are shifted by a constant for clarity. Spectra along two other directions for  $n = 1.15$  are also shown: (c)  $(0, 0) - (\pi, \pi)$  and (d)  $(0.65\pi, 0) - (0.65\pi, \pi)$ . The corresponding experimental data are in Fig. 2 of Ref. [7] and Fig. 1 of Ref. [6]. Band parameters  $t' = -0.175t$ ,  $t'' = 0.05t$ ,  $t = 350$  meV, while  $T = t/20$ .

intersection of the Fermi surface with the AFM zone boundary. Throughout this Letter, we present results for  $t' = -0.175t$  and  $t'' = 0.05t$ , but very similar results are obtained for another choice of parameters [4]  $t' = -0.275t$  and  $t'' = 0.0$  [21]. There are no phenomenological parameters, such as mode coupling constants or additional renormalizations of  $U$ , as can occur in other theories. For actual comparisons with experiment, we take  $t = 350$  meV [22] since this allows us to find agreement with the experimentally observed overall ARPES dispersion.

We present in Fig. 1 the single-particle spectral weight for two fillings,  $n = 1.15$  and  $1.10$ . Here,  $A(\vec{k}, \omega)$  is multiplied by the Fermi-Dirac distribution function  $f(\omega)$  to allow direct comparison with experiment on  $\text{Nd}_{2-x}\text{Ce}_x\text{CuO}_4$  ( $n = 1 + x$ ) [6,7]. One should also recall that experimental data contain a background at large binding energy whose origin is most probably extrinsic [23]. The results that we present, Figs. 1, 2(a), and 2(b), are at temperature  $T = t/20$  (200 K) that is high compared with phase transitions [8] but that is below the pseudogap temperature  $T^*$ . We have verified that they remain essentially unchanged [24] as  $T$  is decreased towards the range where experiments have been performed [6,7].

Our results for 15% doping [Fig. 1(a)] are in remarkable agreement with ARPES data on reduced  $e$ -doped cuprates [6,7] when we use  $U = 5.75t$ . In ARPES, superconductivity leads only to a 2 meV shift of the leading edge [6] so it would not be observable on the scale of Fig. 1. We see that  $A_<(\vec{k}_F, \omega)$  is peaked near  $(\pi, 0)$  and  $(\pi/2, \pi/2)$  and is pseudogapped at hot spots. Smaller values of  $U$  can be below the critical  $U_c$  necessary for spin fluctuations to build up in the presence of frustrating  $t'$  and  $t''$ . At  $U = 5.25t$ , for instance, sharp quasiparticle peaks appear everywhere along the Fermi surface (not shown here). For larger  $U$ , the spectral weight  $A_<(\vec{k}_F, \omega)$  is strongly suppressed near  $(\pi/2, \pi/2)$  because scattering by spin fluctuations is stronger and extends over a broader region in  $\mathbf{k}$  space [3]. For 10%  $e$ -doped cuprates, on the other hand, the best fit to experiments is found for  $U = 6.25t$  [Fig. 1(b)], not for  $U = 5.75t$ . At  $U = 6.25t$  the weight  $A_<(\vec{k}_F, \omega)$  near  $(\pi/2, \pi/2)$  is shifted away from the

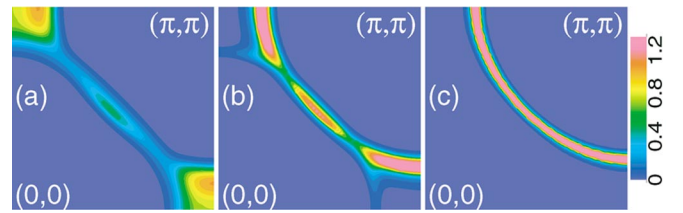


FIG. 2 (color). Fermi surface plot for (a)  $U = 6.25t$ ,  $n = 1.10$ ,  $T = t/20$ , (b)  $U = 5.75t$ ,  $n = 1.15$ ,  $T = t/20$ , and (c)  $U = 5.75t$ ,  $n = 1.20$ ,  $T = t/50$ . See the corresponding experimental plots in Fig. 3 of Ref. [7].

Fermi energy (pseudogap), in good agreement with the experimental results [7], while at  $U = 5.75t$  (not shown here), a pseudogap would not appear near  $(\pi/2, \pi/2)$  [25]. An increase of  $U$  with decreasing doping is also expected from the fact that  $U = 6.25t$  is not large enough to produce the observed [26] Mott gap at half filling. Our calculated  $A_{<}(\vec{k}, \omega)$  along some selected directions also agrees well with ARPES data [6]. Along  $(0, 0) - (\pi, \pi)$  [Fig. 1(c)] a sharp peak approaches the Fermi energy near  $\vec{k}_F$ , while along  $(0.65\pi, 0) - (0.65\pi, \pi)$  [Fig. 1(d)] the peak does not go through the Fermi energy and seems to bounce back near  $\vec{k}_F$ . The peak position where bouncing occurs may be used to obtain a rough estimate of pseudogap size  $\Delta_{PG}$ . For 15% and 10% dopings we find about 0.1 and 0.3 eV, respectively.

Calculated Fermi surface plots  $A_{<}(\vec{k}, 0)$  are obtained by integrating  $A(\vec{k}, \omega)f(\omega)$  in a window  $(-0.2t, 0.1t)$ , comparable to that of experiment [7]. The overall features are not sensitive to this choice for the parameters used here. For 10% doping [Fig. 2(a)], strong AFM fluctuations cause the suppression of spectral weight not only at hot spots, but also along a large segment of the Fermi surface near  $(\pi/2, \pi/2)$ . As a consequence, at 10% doping the Fermi surface plot looks as if it was composed of pockets near  $(\pi, 0)$ . As shown in Fig. 2(b), for 15% doping the spectral weight at  $\omega = 0$  is strongly suppressed by AFM fluctuations only at hot spots. All these results are observed in ARPES data [6,7] for  $e$ -doped cuprates. These features follow from  $\vec{k}$  dependent scattering rates due to AFM fluctuations.

*Pseudogap temperature and quantum critical point.*— Within TPSC, it has been predicted analytically that the pseudogap in the spectral function occurs at  $T^*$  when points of the two-dimensional Fermi surface can be connected by the AFM wave vector [27] and when  $\xi$  begins to exceed  $\xi_{th} = \hbar v_F / \pi k_B T$  at these points [16,17,27]. The pseudogap is a precursor of the long-range AFM state in two dimensions. Decreasing  $T$  below  $T^*$  increases  $\xi$  beyond  $\xi_{th}$  and does not produce large changes in the spectra [24]. In our calculations, the AFM-induced  $T^*$  ends at the same value of doping as the QCP where  $T = 0$  two-dimensional antiferromagnetism disappears. For  $x$  below the QCP, the  $T = 0$  magnetic order can be commensurate or incommensurate although at  $T^*$  the fluctuations are commensurate. The two-dimensional QCP, which may be masked by a superconducting Kosterlitz-Thouless transition [28] or by three-dimensional ordered phases, is near 18%, much smaller than the naive percolation threshold [8]. At the QCP we find  $\omega/T$  scaling in the self-energy and  $\xi \sim T^{-1/z}$  with dynamical exponent  $z = 2$ . This asymptotically implies  $\xi < \xi_{th}$  and hence there is no pseudogap at the QCP. Figure 2(c) illustrates our prediction that hot spots in  $A_{<}(\vec{k}, 0)$  disappear beyond the QCP even at very low temperature. We are also pre-

dicting that the pseudogap observed in ARPES energy distribution curves at low temperature should persist almost unchanged up to the  $T^*$  indicated by the filled circles in Fig. 3. As temperature increases above  $T^*$ , the pseudogap in energy distribution curves begins to disappear and red segments in Fig. 2 will enlarge gradually until one recovers a continuous Fermi surface at around  $2T^*$ .

The empty circles in Fig. 3 are the observed pseudogap temperatures  $T^*$  extracted from optical conductivity data by Onose *et al.* [13]. These follow closely the  $T^*$  that we predict for ARPES and scales with the observed  $T_N$  curve (approximately 2 times larger) supporting the AFM fluctuation origin of the pseudogap in the normal state of  $e$ -doped cuprates. Onose *et al.* [13] found that  $\Delta_{PG}$  and  $T^*$  satisfy the relation  $\Delta_{PG} \approx 10k_B T^*$ . Our estimation of the ratio of  $\Delta_{PG}$  to  $T^*$  leads to 10 and 7.5 for 10% and 15% dopings, respectively, in rough agreement with the above experiment. Note that  $T^*$  is considerably decreased compared with the mean-field  $T_N$  by both Kanomori screening and thermal fluctuations, two effects taken into account by TPSC.

*Antiferromagnetic correlation length.*—To demonstrate convincingly that our picture is consistent, we need to show that our results also agree with the experimentally observed AFM  $\xi$ . Mang *et al.* [8] and Matsuda *et al.* [9] have obtained neutron scattering results for  $\xi(T)$  at various dopings for oxygenated samples of  $Nd_{2-x}Ce_xCuO_4$ . They find an exponential dependence of  $\xi(T)$  on inverse temperature. This is illustrated on an Arrhenius plot in Fig. 4 along with our calculated  $\xi(T)$ . Analytical results for TPSC [15] indeed show that the pseudogap occurs in the renormalized classical regime where the characteristic spin fluctuation energy is less than the thermal energy and where  $\xi(T) \sim \exp(C/T)$  with  $C$  being generally a weakly temperature-dependent constant. The temperature at which  $A_{<}(\vec{k}, \omega)$  has been calculated,  $T = t/20$  denoted by an arrow in Fig. 4, is still in the exponential regime. The value of  $\xi(T)$  at that temperature for optimal doping is 20 to 30 lattice constants (long but finite). For 10% doping (not shown here),

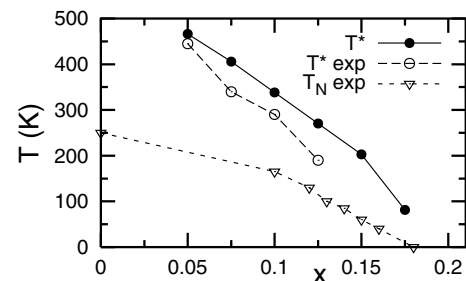


FIG. 3. Pseudogap temperature  $T^*$  (filled circles denote calculated  $T^*$ , empty ones experimental data extracted from optical conductivity [13]). Empty triangles are experimental Néel temperatures  $T_N$ . The samples are reduced [8].

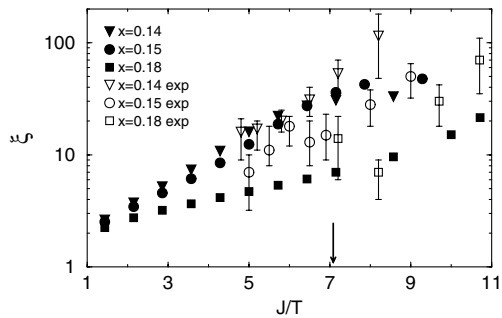


FIG. 4. Semilog plot of the AFM correlation length (in units of the lattice constant) against inverse temperature (in units of  $J = 125$  meV) for  $x = 0.14, 0.15,$  and  $0.18$ . Filled symbols denote calculated results and empty ones experimental data of Refs. [8,9]. The arrow indicates  $T = t/20$  where most spectral quantities in Figs. 1 and 2 are calculated.

the calculated  $\xi(T)$  is also in good agreement at high temperatures but the agreement becomes less satisfactory at low temperatures since the quantitative details of TPSC become less accurate for very large  $\xi$ . Also, one should allow for some small uncertainty in the doping [8] or in the parameters of the Hubbard model because neutron experiments were performed on oxygenated (as grown) samples while ARPES was done on reduced ones [29]. We predict that dynamic neutron scattering will find overdamped spin fluctuations as we enter the pseudogap regime and that the characteristic spin fluctuation energy will be smaller than  $k_B T$  whenever a pseudogap is present. Equality will occur well above  $T^*$ .

*Long-range order.*—In the extended TPSC approach [3] AFM fluctuations can both help and hinder  $d$ -wave superconductivity, depending on the strength of the pseudogap. For the case at hand, a finite  $T_c$  appears below 18% doping and increases with decreasing doping. We cannot study at this point the effect of the appearance of long-range Néel order on superconductivity, but the estimated value of  $T_c$  near optimal doping is roughly the experimental result [6,12]. By adding hopping  $t_z = 0.03t$  in the third direction, we also find a Néel temperature that is in fair agreement with the experimental data by Mang *et al.* [8] for  $x \geq 0.14$ .

In conclusion, we have shown that ARPES spectra [6,7] and the antiferromagnetic correlation length obtained by neutron scattering [8,9] in  $e$ -doped cuprates can all be theoretically explained in detail within the Hubbard model in the weak to intermediate coupling regime. We have made several predictions for future experiments. The physical picture of the normal state that emerges is that of electrons on a planar lattice scattering off quasistatic antiferromagnetic fluctuations. These have large phase space in two dimensions so that quasiparticles in regions of the Fermi surface that can be connected by the antiferromagnetic wave vector do not survive scattering by these low-energy bosons [16,27,30]. The electron-doped

cuprates appear to be the first high-temperature superconductors whose normal state lends itself to such a detailed theoretical description.

We acknowledge useful discussions with N.P. Armitage, P. Fournier, M. Greven, R.S. Markiewicz, Y. Onose, M. Rice, D. Sénéchal, and L. Taillefer. The present work was supported by NSERC Canada, by FQRNT Québec, by CIAR, and by the Tier I Canada Research Chair Program (A.-M. S.T.). A.-M. S.T. acknowledges the hospitality of Université de Provence and of Yale University where part of this work was performed and, in the latter case, supported under NSF Grant No. 0342157.

- [1] A. Damascelli *et al.*, *Rev. Mod. Phys.* **75**, 473 (2003).
- [2] C. Kusko *et al.*, *Phys. Rev. B* **66**, 140513 (2002).
- [3] B. Kyung *et al.*, *Phys. Rev. B* **68**, 174502 (2003).
- [4] R. S. Markiewicz, cond-mat/0312594 [*Phys. Rev. B* (to be published)].
- [5] D. Sénéchal *et al.*, *Phys. Rev. Lett.* **92**, 126401 (2004).
- [6] N. P. Armitage *et al.*, *Phys. Rev. Lett.* **87**, 147003 (2001).
- [7] N. P. Armitage *et al.*, *Phys. Rev. Lett.* **88**, 257001 (2002).
- [8] P. K. Mang *et al.*, *Phys. Rev. Lett.* **93**, 027002 (2004).
- [9] M. Matsuda *et al.*, *Phys. Rev. B* **45**, 12 548 (1992).
- [10] T. Tohyama *et al.*, *Phys. Rev. B* **64**, 212505 (2001).
- [11] H. Kusunose *et al.*, *Phys. Rev. Lett.* **91**, 186407 (2003).
- [12] G. Blumberg *et al.*, *Phys. Rev. Lett.* **88**, 107002 (2002).
- [13] Y. Onose *et al.*, *Phys. Rev. Lett.* **87**, 217001 (2001).
- [14] Y. Dagan *et al.*, *Phys. Rev. Lett.* **92**, 167001 (2004).
- [15] Y. M. Vilks *et al.*, *Phys. Rev. B* **49**, 13 267 (1994).
- [16] Y. M. Vilks *et al.*, *J. Phys. I (France)* **7**, 1309 (1997).
- [17] S. Moukouri *et al.*, *Phys. Rev. B* **61**, 7887 (2000).
- [18] S. Allen *et al.*, in *Theoretical Methods for Strongly Correlated Electrons*, edited by D. Sénéchal *et al.* (Springer, New York, 2003).
- [19] A. F. Veilleux *et al.*, *Phys. Rev. B* **52**, 16 255 (1995).
- [20] B. Kyung *et al.*, *Phys. Rev. Lett.* **90**, 099702 (2003).
- [21] We do not claim three digit accuracy in our choice of parameters. We generally tried several values separated by  $0.025t$ . The two sets of band parameters quoted correspond to local “best choices.”
- [22] C. Kim *et al.*, *Phys. Rev. Lett.* **80**, 4245 (1998).
- [23] A. Kaminski *et al.*, *Phys. Rev. B* **69**, 212509 (2004).
- [24] Spectral peaks at  $\omega = 0$  near  $(0, \pi)$  become sharper in qualitative agreement with recent experiments by Y. Onose *et al.* *Phys. Rev. B* **69**, 024504 (2004).
- [25] One would need an unrealistic 20% change in hopping  $t'$  to keep  $U$  identical at  $n = 1.1$  and  $n = 1.15$ .
- [26] S. Uchida *et al.*, *Physica (Amsterdam)* **162C**, 1677 (1989).
- [27] Y. M. Vilks, *Phys. Rev. B* **55**, 3870 (1997).
- [28] When this occurs, additional superconducting precursor effects may contribute to the pseudogap.
- [29] V. Hankevych *et al.*, cond-mat/0407085.
- [30] Y. M. Vilks *et al.*, *J. Phys. Chem. Solids* **56**, 1769 (1995); *Europhys. Lett.* **33**, 159 (1996).